

1 **Supporting Information for: Altimeter-Era Emergence of the Patterns**  
2 **of Forced Sea Level Rise in Climate Models and Implications for the**  
3 **Future**

4  
5 **John T. Fasullo<sup>1,2\*</sup>, R. Steven Nerem<sup>2</sup>**

6  
7  
8 <sup>1</sup>National Center for Atmospheric Research, Boulder, CO, USA

9 <sup>2</sup>Smead Aerospace Engineering Sciences, Colorado Center for Astrodynamics  
10 Research, Cooperative Institute for Research in Environmental Sciences, University  
11 of Colorado, Boulder, CO, USA

12  
13 \*Corresponding author: [fasullo@ucar.edu](mailto:fasullo@ucar.edu)

14  
15 *in revision at PNAS*

16  
17  
18 Phone: (303) 497 1712

19 Fax: (303) 497 1333

20  
21 Oct 2018  
22  
23  
24  
25

---

<sup>1</sup> NCAR is sponsored by the National Science Foundation.

26  
27  
28  
29  
30  
31  
32  
33  
34  
35  
36  
37  
38

The following material is supporting information for “**Altimeter-Era Emergence of the Patterns of Forced Sea Level Rise and Implications for the Future**” by J. T. Fasullo and R. S. Nerem. It is comprised of 2 tables and 11 figures.

39 **Tables**

40

41 **Table S1: Pattern correlations between ensemble-mean regional sea level trends for**  
 42 **JJA and DJF in CESM and ESM2M across various periods. Patterns for the**  
 43 **altimeter era CESM seasonal trends are shown in Fig. SA.**

44

JJA-DJF PCs	CESM	ESM2M
<b>1950-2100</b>	<b>0.97</b>	<b>0.99</b>
<b>1950-1975</b>	<b>0.91</b>	<b>0.98</b>
<b>1993-2018</b>	<b>0.91</b>	<b>0.99</b>
<b>2020-2045</b>	<b>0.95</b>	<b>0.99</b>

45

46 **Table S2: Table 2: Representativeness of Long Term Pattern: Pattern correlations**  
 47 **between the long-term FR (1950-2100) in sea level with other time periods in**  
 48 **ESM2M for the global ocean and by basin. The correlations demonstrate the**  
 49 **similarity between simulated altimeter-era, and near future (2020-45) FR**  
 50 **patterns of rise while highlighting the change in those patterns from the mid-20<sup>th</sup>**  
 51 **Century.**

52

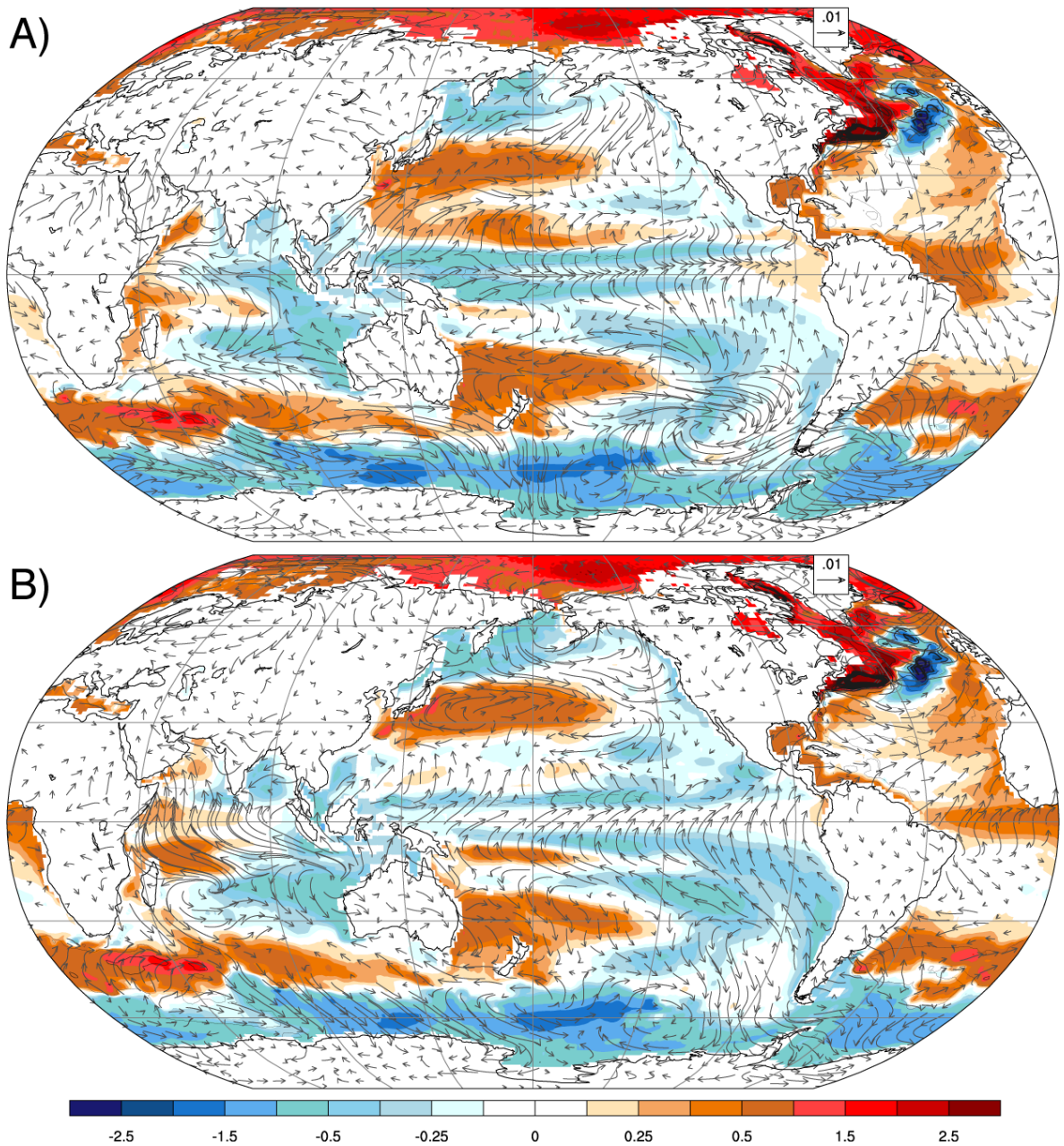
	ESM2M				
	Global	Atlantic	Southern	Pacific	Indian
<b>1950-1975</b>	<b>-0.02</b>	<b>0.20</b>	<b>-0.31</b>	<b>-0.20</b>	<b>-0.18</b>
<b>1993-2018</b>	<b>0.84</b>	<b>0.77</b>	<b>0.86</b>	<b>0.85</b>	<b>0.88</b>
<b>2020-2045</b>	<b>0.92</b>	<b>0.90</b>	<b>0.93</b>	<b>0.93</b>	<b>0.93</b>

53

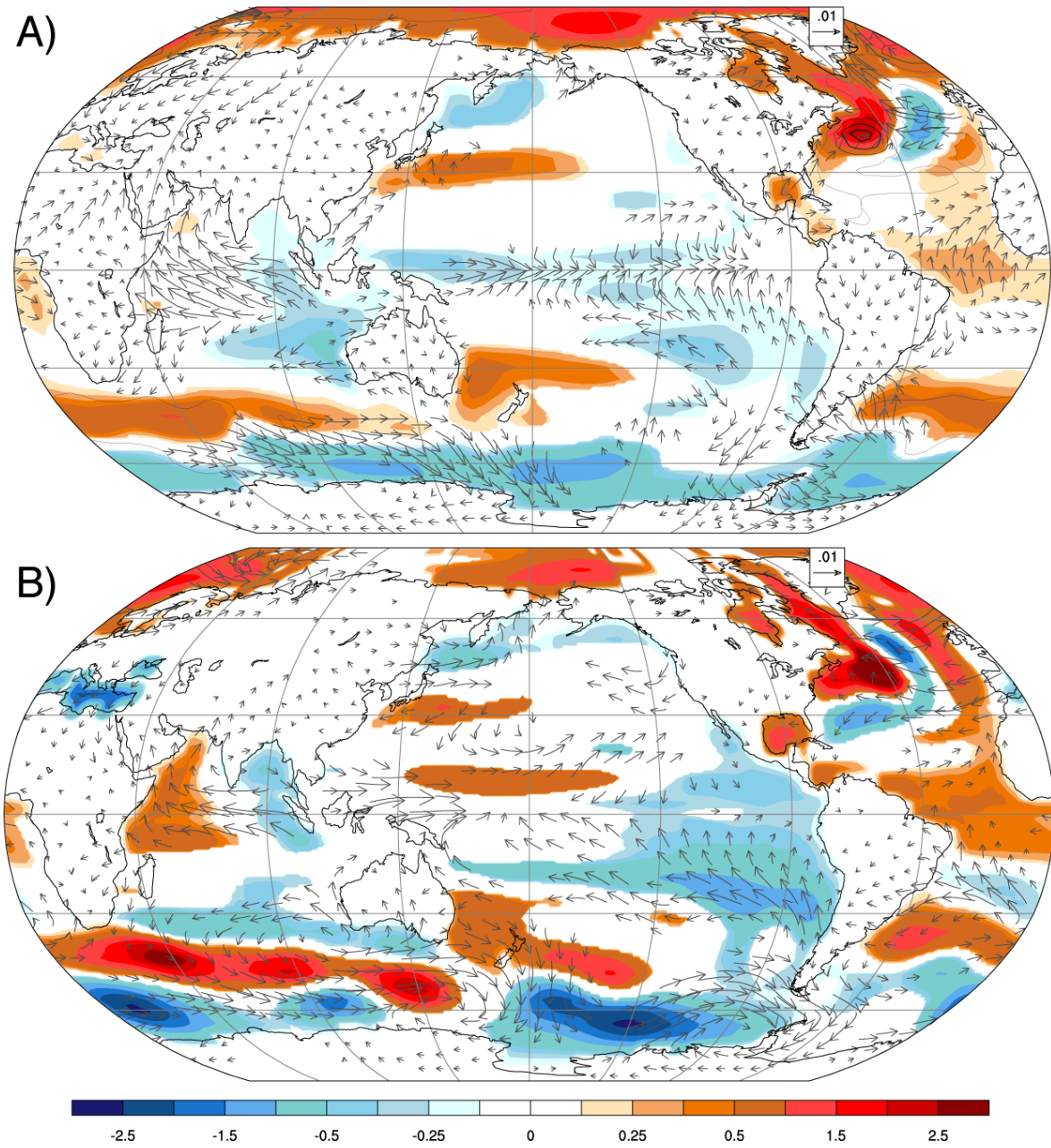
54

55

56 **Figures**  
57  
58  
59

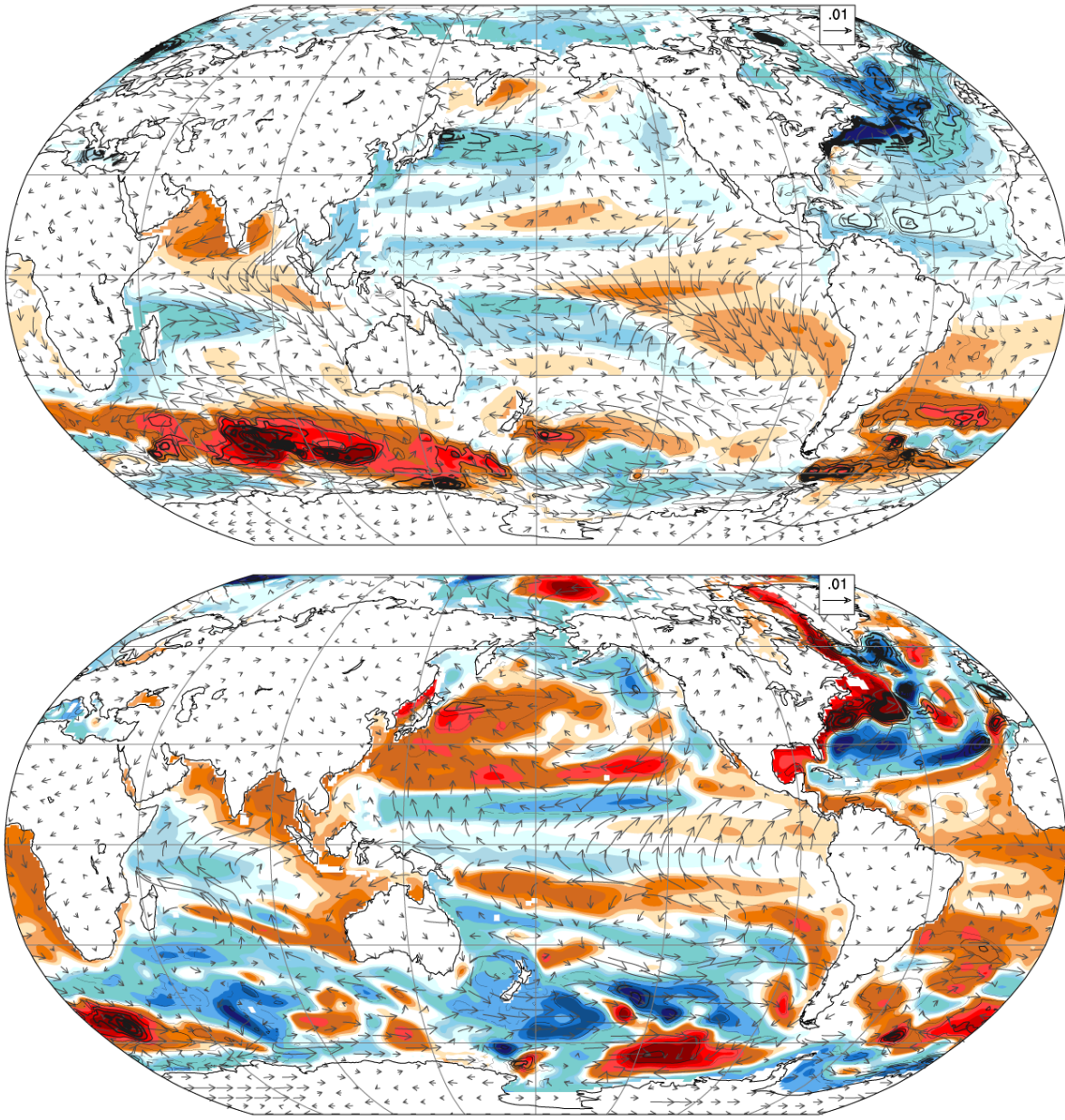


60  
61 **Fig. S1: Seasonal patterns (JJA, A, and DJF, B) of the CESM 1993-2018 forced**  
62 **response in relative sea level (global mean removed) and near-surface winds**  
63 **(vectors,  $\text{m s}^{-1} \text{ yr}^{-1}$ ).**  
64



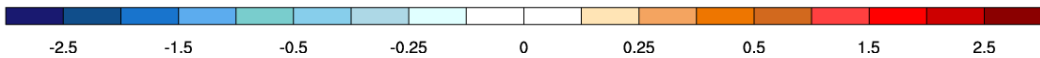
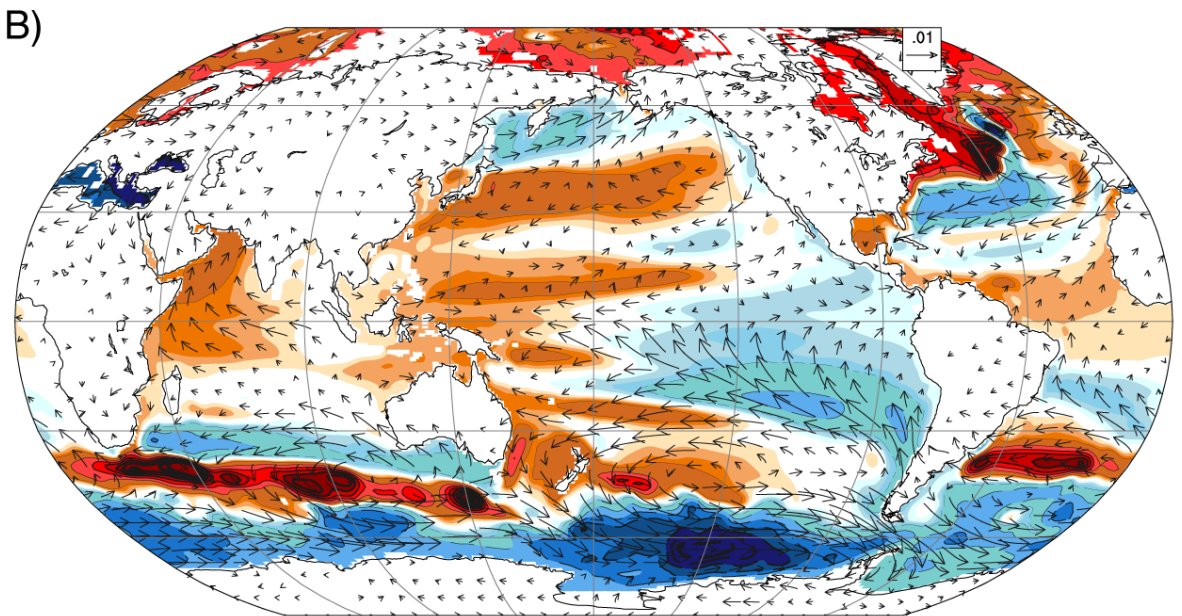
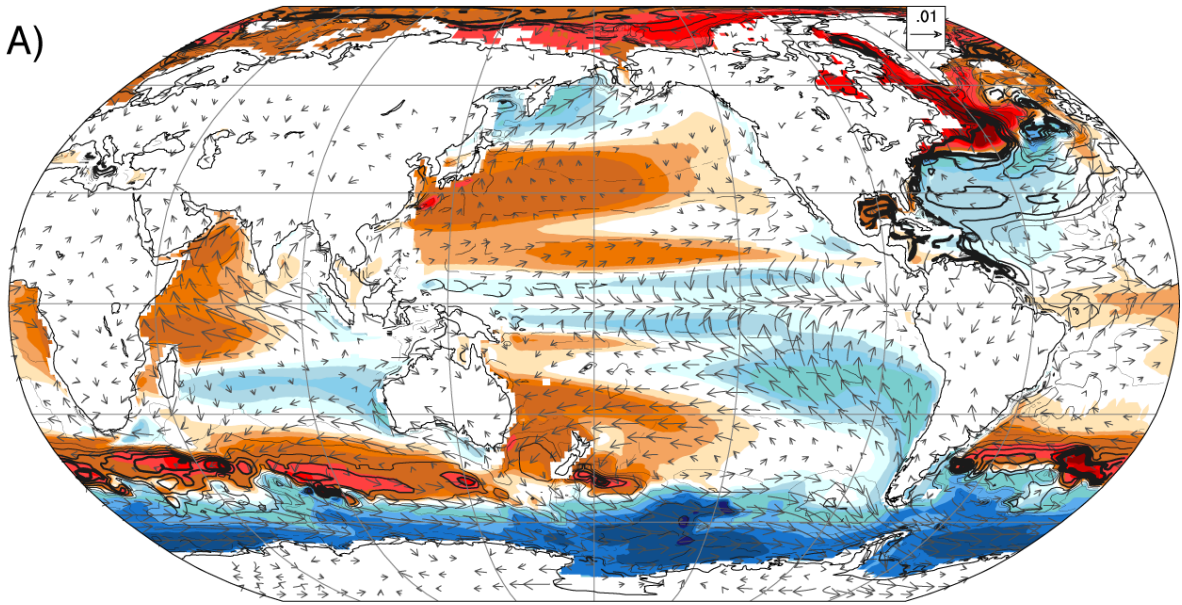
65  
66  
67  
68  
69  
70  
71

**Figure S2: Statistically significant relative sea level forced response trends in  $\text{mm yr}^{-1}$  from 1993-2018 (global mean removed) for the CESM (A) and ESM2M (B). Significant trends in surface winds are also shown (vectors,  $\text{m s}^{-1} \text{yr}^{-1}$ ). Only fields where  $|p| < 0.05$  are shown, based on regions where the FR exceeds twice the ensemble standard error.**



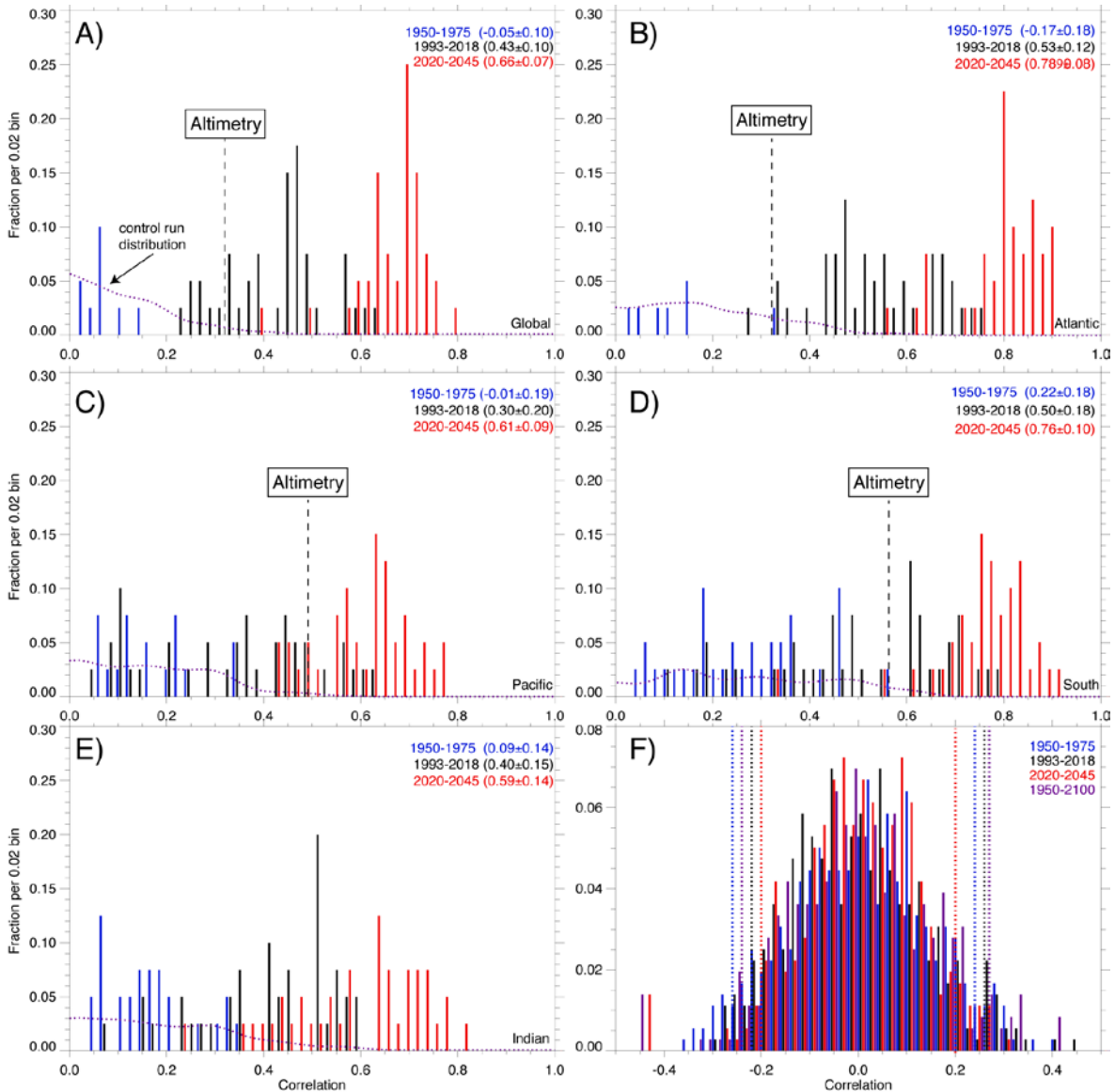
72  
73  
74  
75

**Figure S3: The forced response from 1950 to 1975 in relative sea level (mm/y, global mean removed) and near-surface winds (m/s/y) based on ensemble-mean trends in the CESM (A) and ESM2M (B).**



76  
77  
78  
79  
80

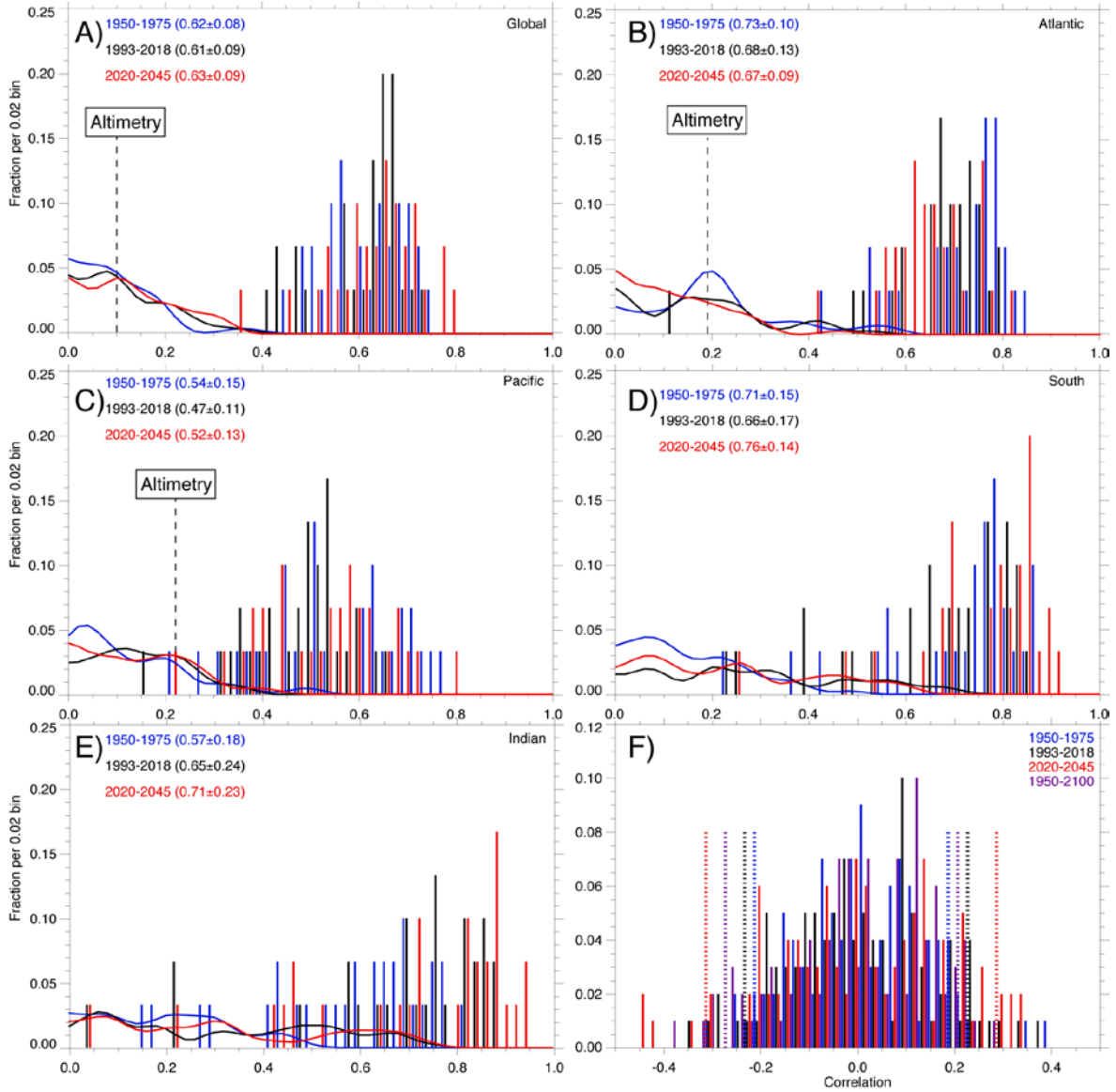
**Figure S4: Forced response in relative sea level (mm/y, global mean removed) and near surface winds (m/s/y) from 1950 to 2100 based on ensemble-mean trends in CESM (A) and ESM2M (B).**



81  
82  
83  
84  
85  
86  
87  
88  
89  
90  
91  
92  
93  
94  
95

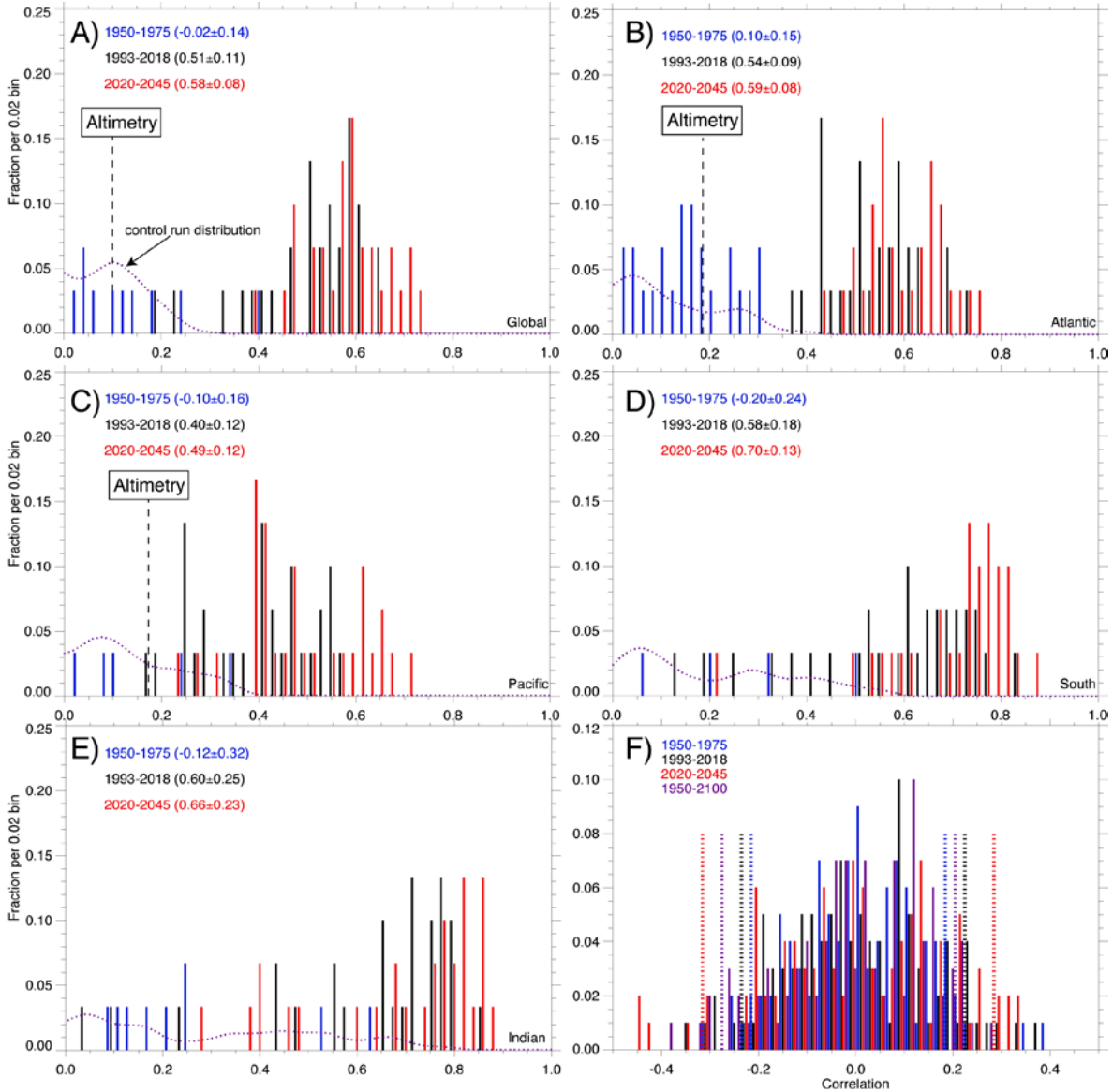
**Fig. S5: Histograms of the fractional occurrence of pattern correlations in the CESM LE of individual member trends across various eras with the 1950-2100 FR for A) the global ocean, and B) the Atlantic, C) Pacific, D) Southern, and E) Indian Ocean basins (associated ocean boundaries shown in Fig. 1A). Dotted lines in A-E correspond to occurrences obtained at random in the control run (shown in detail for the global ocean in F). Dashed lines in (F) correspond to 95% confidence intervals for pattern correlations in the control run. Also shown in A-D are the pattern correlations of the 1950-2100 FR with observed altimeter-era trends, smoothed to T42 spectral wavenumbers, omitted for the Indian Ocean where the correlation is negative (-0.03). Plotted fractional occurrence in A-E does not sum to unity where members with negative correlations exist (e.g. 1950-75 in A).**





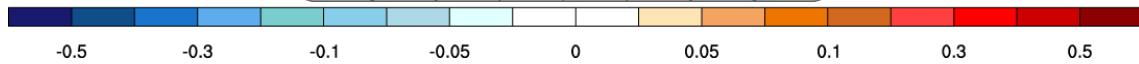
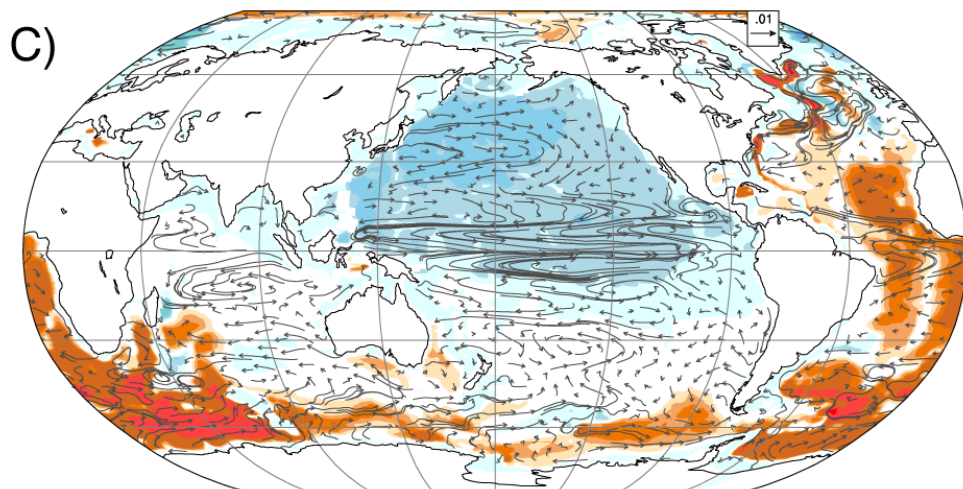
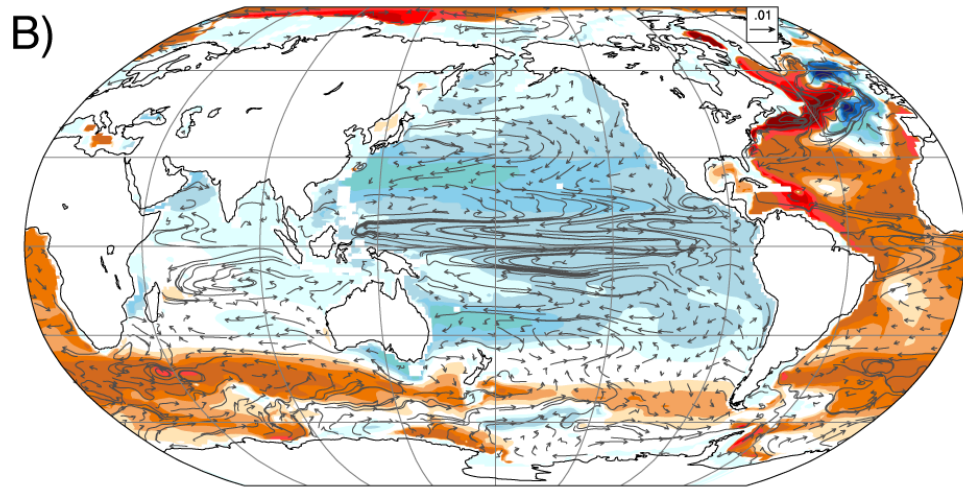
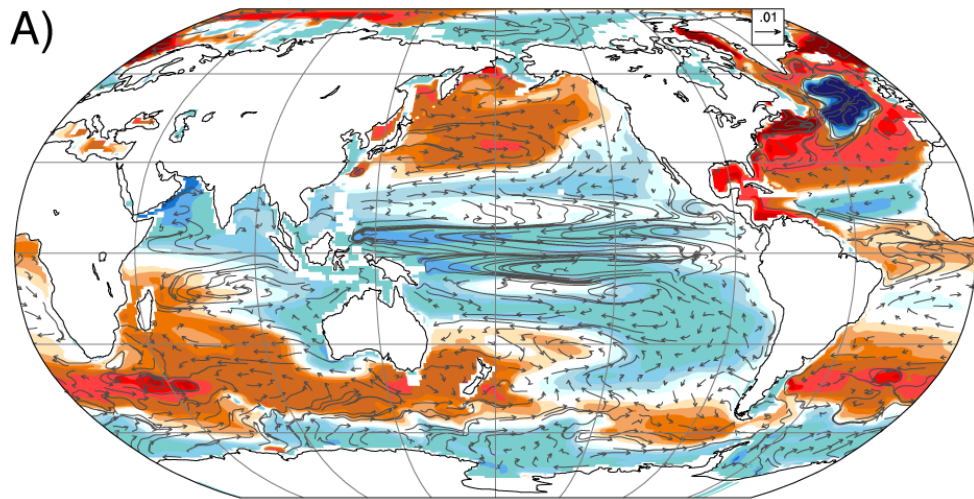
98  
99  
100  
101  
102  
103  
104  
105  
106  
107  
108  
109  
110  
111

**Fig. S6: Histograms of the fractional occurrence of pattern correlations in the ESM2M LE of individual member trends across various eras with the contemporaneous FRs for A) the global ocean, and B) the Atlantic, C) Pacific, D) Southern, and E) Indian Ocean basins (associated ocean boundaries shown in Fig. 1A). Colored lines in A-E correspond to occurrences obtained for the three eras' FR from the control run (for the globe shown in detail in F). Dashed lines in (F) correspond to 95% confidence intervals for pattern correlations in the control run. Also shown in A-C are the pattern correlations of the 1950-2100 forced response with observed altimeter trends, smoothed to T42 spectral wavenumbers, omitted for the Southern and Indian Ocean where the correlations are negative (-.01 and -.27, respectively). Plotted fractional occurrence in A-E does not sum to unity where members with negative correlations exist.**



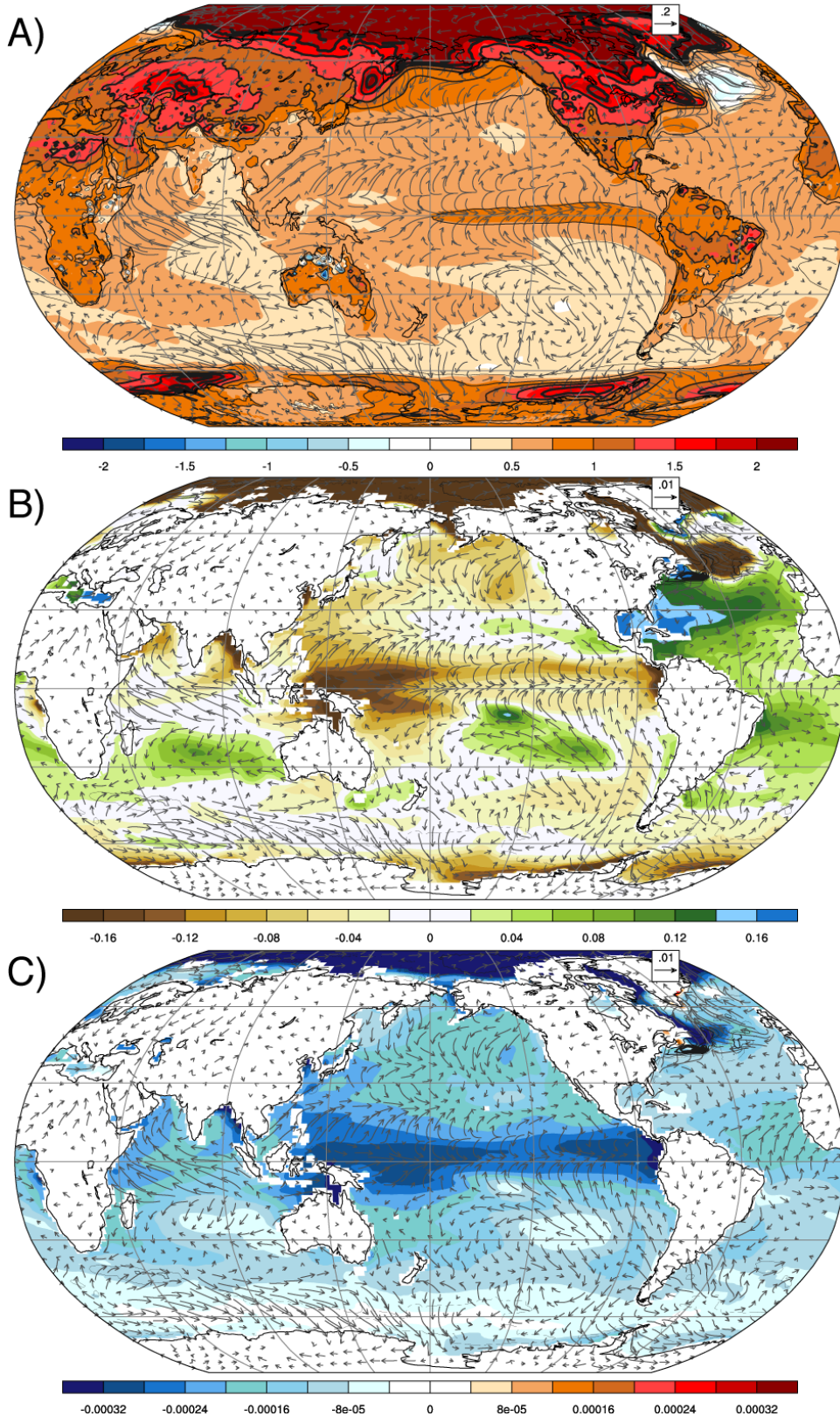
112  
 113  
 114  
 115  
 116  
 117  
 118  
 119  
 120  
 121  
 122  
 123  
 124  
 125  
 126  
 127

**Fig. S7: Histograms of the fractional occurrence of pattern correlations in the ESM2M LE of individual member trends across various eras with the 1950-2100 FR for A) the global ocean, and B) the Atlantic, C) Pacific, D) Southern, and E) Indian Ocean basins (associated ocean boundaries shown in Fig. 1A). Dotted lines in A-E correspond to occurrences obtained at random in the control run (shown in detail for the global ocean in F). Dashed lines in (F) correspond to 95% confidence intervals for pattern correlations in the control run. Also shown in A-C are the pattern correlations of the 1950-2100 FR with observed altimeter-era trends, smoothed to T42 spectral wavenumbers, omitted for the Southern and Indian Oceans where the correlations are negative (-0.01 and -0.20, respectively). Plotted fractional occurrence in A-E does not sum to unity where members with negative correlations exist (e.g. 1950-75 in A).**



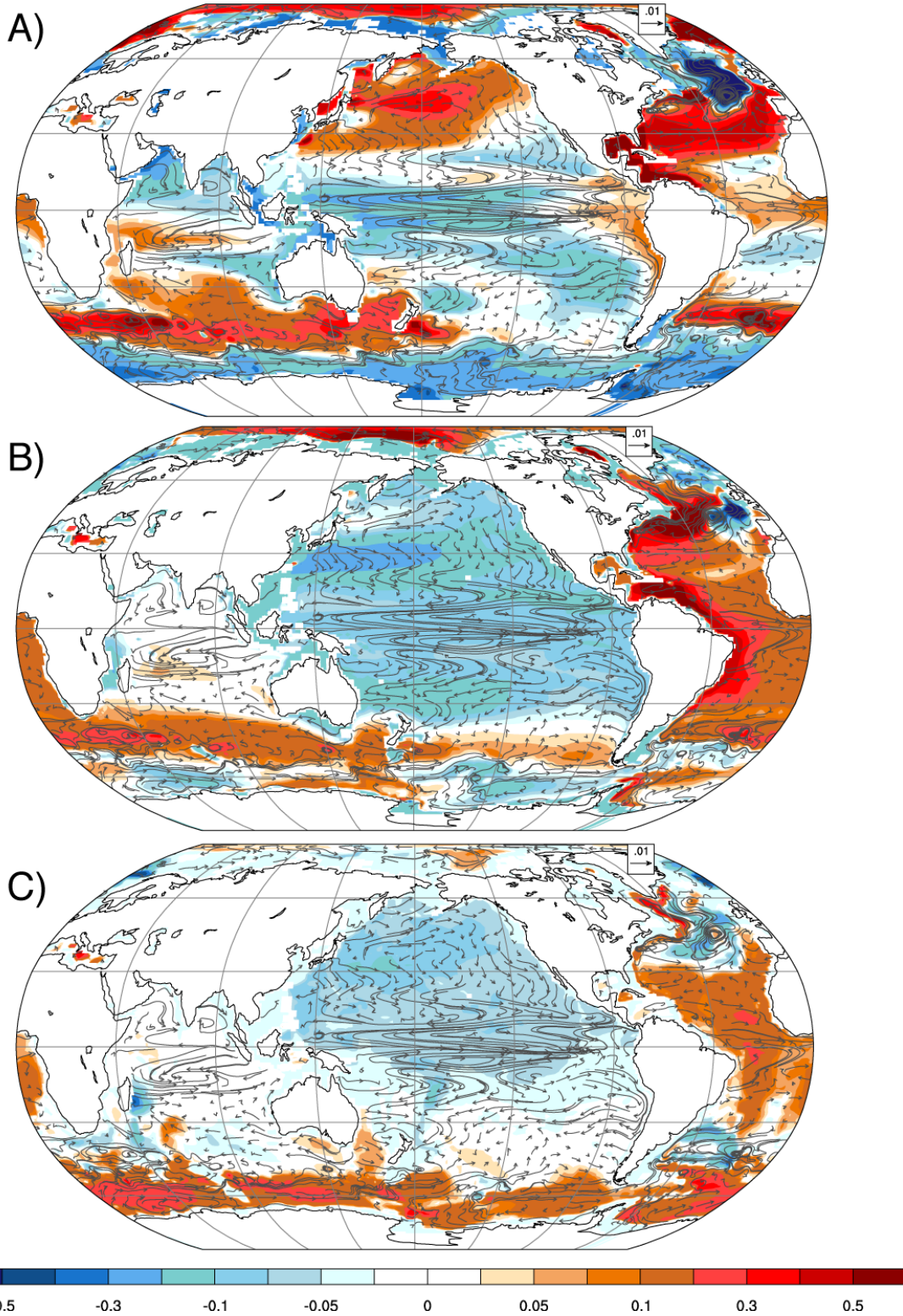
128  
129  
130  
131  
132

**Figure S8: Trends in relative ocean heat content (global mean removed) by depth ( $10^8 \text{ J/m}^2/\text{y}$ ) during the altimeter era for the CESM forced response. Depths include 0-700 m (A), 700-2000m (B), and below 2000m (C). Also shown are trends in surface currents (vectors, cm/s/y).**



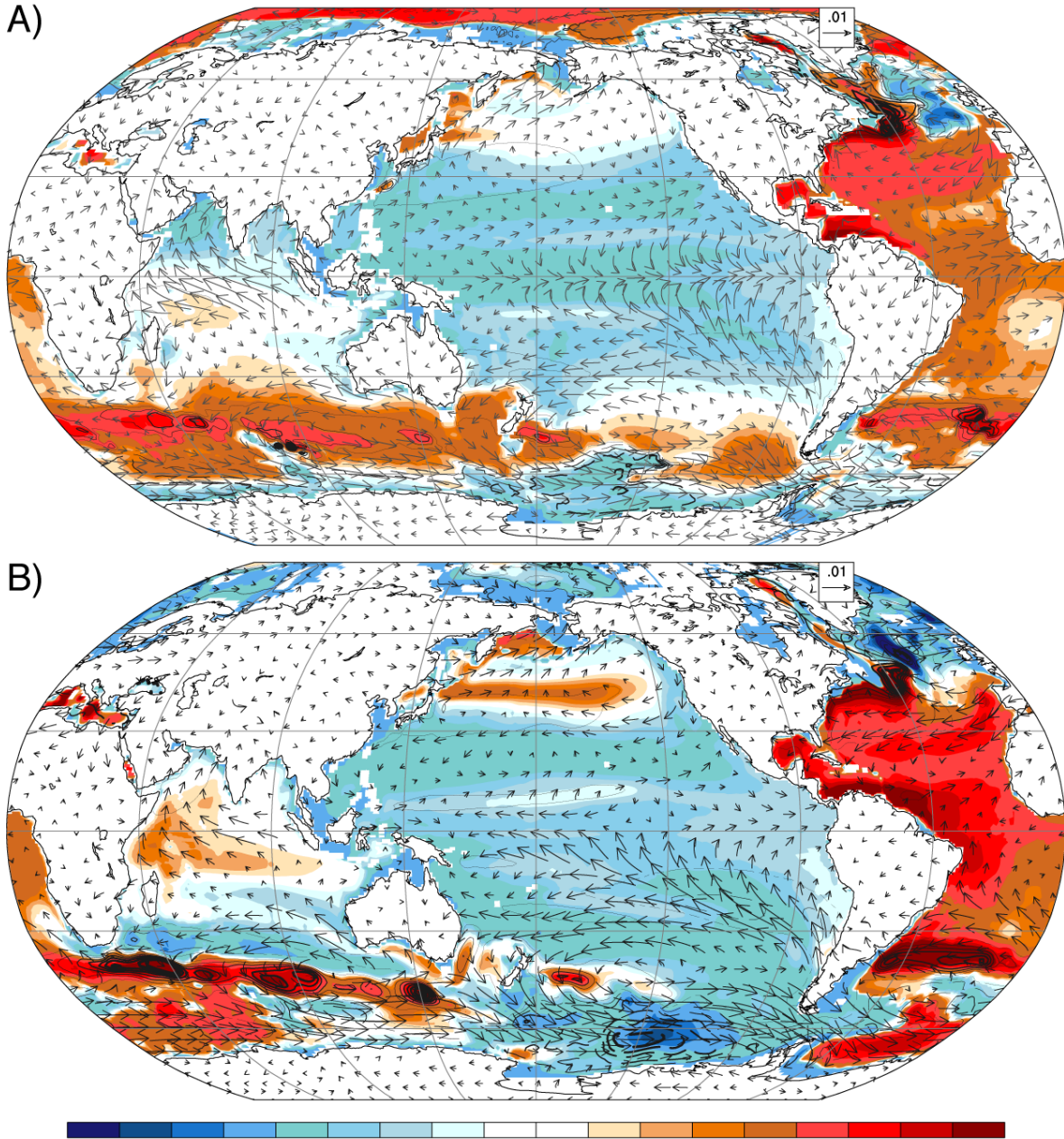
133  
134  
135  
136

**Figure S9: Altimeter-era trends in surface temperature (A, K), salinity (B, g/kg), and potential density (C, kg/kg) for the CESM forced response. Vectors show the forced response trends in near surface winds (m/s/y).**



138  
 139  
 140  
 141  
 142

**Figure S10: Trends in relative ocean heat content (global mean removed) by depth ( $10^8 \text{ J/m}^2/\text{y}$ ) from 2020-2045 for the CESM forced response. Depths include 0-700 m (A), 700-2000m (B), and below 2000m (C). Also shown are trends in surface currents (vectors,  $\text{cm/s/y}$ ).**



143  
 144  
 145  
 146  
 147

**Figure S11: The forced response from 1950-2100 in relative (global mean removed) ocean heat content (filled contours,  $10^8 \text{ J y}^{-1}$ ) and sea level (contour lines,  $0.5 \text{ mm y}^{-1}$  intervals) for the CESM (A) and ESM2M (B) ensemble means.**